Static states and dynamic behaviour of charges: observation and control by scanning probe microscopy

2010 J. Phys.: Condens. Matter 22 173001

(http://iopscience.iop.org/0953-8984/22/17/173001)

IOP Publishing Journal of Physics: Condensed Matter

J. Phys.: Condens. Matter **22** (2010) 173001 (12pp) doi:10.1088/0953-8984/22/17/173001

TOPICAL REVIEW

Static states and dynamic behaviour of charges: observation and control by scanning probe microscopy

Masashi Ishii

National Institute for Materials Science (NIMS), 1-2-1 Sengen, Tsukuba, Ibaraki 305-0047, Japan

E-mail: ISHII.Masashi@nims.go.jp

Received 26 February 2010
Published 29 March 2010
Online at stacks.iop.org/JPhysCM/22/173001

Abstract

This paper reviews charges that locally functionalize materials. Microscopic analyses and operation of charges using various scanning probe microscopy (SPM) techniques have revealed static, quasi-static/quasi-dynamic and dynamic charge behaviours. Charge-sensitive SPM has allowed for the visualization of the distribution of functionalized charges in electronic devices. When used as bit data in a memory system, the charges can be operated by SPM. The behaviour of quasi-static/quasi-dynamic charges is discussed here. In the data-writing process, spatially dispersive charges rather than a fast injection rate are introduced, but the technical problems can be solved by using nanostructures. Careful charge operations using SPM should realize a memory with a larger density than Tbit/inch^2. Dynamic charges have been introduced in physical analyses and chemical processes. Although the observable timescale is limited by the SPM system response time of the order of several seconds, dynamics such as photon-induced charge redistributions and probe-assisted chemical reactions are observed.

Contents

1. Introduction

1.1. Macroscopic measurement of charges

Charges are the origin of the functionalities of electronic and optical devices. In order to fabricate novel devices, considerable time has been spent analysing and controlling charges exhibiting various behaviours such as static, quasi-static and dynamic motions.

A few decades ago, we attempted to fabricate Si and a few compound semiconductors with perfect crystallinity, high purity and well-controlled doping states; all of these crystal fields directly determine the properties of charges such as the mobility and lifetime of a carrier [1, 2]. In particular, there are many types of defects that are accidentally introduced into semiconductor crystals, which trap free carriers and degenerate the inherent functionalities of the constructed

device structures. A large amount of research has contributed towards clarifying the electronic states of these defects [3, 4], identifying their local structures [5, 6] and inventing new processes for suppressing the defects [7, 8]. These research activities have greatly contributed to progress in the large-scale integration of semiconductors.

In these works, contributions towards measuring capacitance were extremely significant; these include capacitance–voltage measurement, deep-level transient spectroscopy (DLTS) and isothermal capacitance transient spectroscopy (ICTS) [8–12]. These developments were remarkable because, although these measurements can be performed using basic device structures such as the Schottky barrier diode [1], they can be used to investigate the trapped charges selectively and directly. In these measurements, large sample sizes (on the scale of micrometres to millimetres) of evaporated metals are preferable to evaluate many types of traps simultaneously [13] and to estimate the density of each trap. Therefore, macroscopic capacitance measurements using large electrodes were the standard measurement method before the development of scanning probe microscopy (SPM) dedicated to local trap analyses. As shown later, local measurements by SPM drastically decreased the observable size of the capacitor to the nanometre level while maintaining easy operation. However, capacitance measurements that have a history as long as semiconductor devices are used as a basic tool for charge analyses, and the accumulated knowledge on traps is frequently applied to local analyses using SPM techniques [14].

1.2. Macroscopic operations of charges

We now discuss the background of the development of SPM. Although attempts to functionalize the defects in some specific structures were carried out, success was limited to several cases [15–18]. Successful functionalizations were achieved through photo-induced phenomena of a type of defect known as persistent photoconductivity (PPC) effect [19]; the exposure of an insulating sample resulting from the reduction of free carriers at cryogenic temperatures to light produces a high carrier concentration, which persists even after the light is removed. Consequently, the charge operations on defects introduced in a macroscopic region do not have the potential for general device applications.

SPM was established as a visualization technique for the inactive charges in defects; it was immediately extended to the activation of charges; further, it can be used to visualize active charges. The charges in defects are not inactive trapped particles, but can be rearranged, observed and transferred to arbitrary positions as active particles with functionality. The historical research was on defect functionalization and their application to devices which effloresce by the SPM technique.

1.3. Scanning probe microscopy to be dealt with in this review

In this review, we concentrate on the behaviours of charges in a microscopic region observed by SPM. Static, quasi-static and dynamic charges are observed at this scale. Note that these charge behaviours have already been described in the first part of section 1; SPM is closely related to the functionalization of microscopic sites, which is why it was chosen as the topic of this review.

The most common and powerful SPM technique is scanning tunnelling microscopy (STM), which includes scanning tunnelling spectroscopy (STS) using an STM static probe; however, it is not discussed in detail in this review. STM probes the tunnel current, constructs topographic images by electrically conducted surface tracing and spectrally analyses the density of states of an object using the current; thus, it is dependent on the applied bias voltage. Basically, during measurements, charges are continuously flowing between the sample and tip as the tunnel current. The interactive charges observed by STM have already left the materials and are not at work. Therefore, the charges in the tunnel current are different from the charges observed in the area of our interest, i.e. functional charges in microscopic regions. Moreover, although static charges mostly accumulate in insulators, as will be discussed later, STM cannot be used to observe insulators. Therefore, STM was concluded to be inappropriate for our study. However, STM does have many useful applications, and many defects with charge trapping states have been detected by STM [20–23].

There are high expectations for using SPM as an analysis tool to visualize charge distributions for actual devices [24–30]. The SPM microcantilever should be able to observe weak and local electric forces generated by the charges. However, a large number of detection techniques depend on the sample conditions. The great variety in detection techniques reflects the fact that there are many physical parameters related to charges, e.g. capacitance, dielectric constant, electrostatic force, Kelvin force, etc. SPM techniques for probing these physical parameters include scanning capacitance microscopy (SCM or SCaM) [24], electrostatic microscopy (EFM) [25], scanning Kelvin potential microscopy (SKPM) (also known as Kelvin force microscopy (KFM), surface potential microscopy (SSPM)) [26–29] and scanning nonlinear dielectric constant microscopy (SNDM) [30]. An indirect but sensitive observation of charge depletion or accumulation via friction force is also reported [31, 32]. In the following review on charge observation and operations, these techniques appear randomly in various sections. For the same technique with different names such as SKPM, KFM and SSPM, the name used in each reviewed paper is adopted. Basically, charge observations should be performed using a technique appropriate for the sample species, while charge operations are commonly performed with external fields; an example of this is electric bias applied to the tip of the scanning probe and photo/thermal excitations independent of the technique [33–35]. The charge operations that are the main topic of this review are independent of the SPM technique. The details of each SPM technique can be found in technical books [36, 37].

2. Observation of static charges

2.1. Charge distribution at heterojunction

SPM has been successfully applied for observing static charges in various materials. Charge distributions can be observed

by using SPM because it has a higher spatial resolution than conventional techniques. Its abilities have been reviewed in many papers, some of which are discussed below. Note the dimension of objects in each paper discussed. These are not the actual spatial resolution of the SPM techniques, but we can roughly estimate the potential for microscopic charge observation and operation in the SPM techniques.

The basis of semiconductor devices is heterojunctions of materials with different Fermi levels [1, 2]; this produces an electric potential barrier with a depletion layer or potential valley that accumulates charges, resulting in nonlinear conductivity. Therefore, heterojunctions have been under intensive study since the transistor was introduced in 1948. With the present semiconductor integration technology using nanometre-scale devices, KFM is a powerful tool for visualizing the electric potential in a device [38]. Although KFM does not give the charge distribution directly, since charges follow the potential curve, the statistical distribution of charges can be deduced from the image. In other words, KFM reveals a specific electric potential yielding some functionality rather than the functionalized charges. As compared to STM, in KFM, no charge flow is necessary for probe measurements. Even so, the observation of potential curves is somewhat inappropriate for this review topic, similar to STM. However, knowing what related techniques provide is meaningful. In fact, the observable parameter in the KFM technique, the contact potential difference (CPD), which is defined as $\phi_{\mathrm{tip}} - \phi_{\mathrm{sample}}/q$ (where q is the elementary charge, and ϕ_{tip} and ϕ_{sample} are the surface potentials of the tip and sample, respectively) is an absolute value intrinsic to the sample just under the probe. Hence, we can evaluate the objects in a more quantitative manner than the charge observation available for the similar EFM technique. The quantitative evaluation is quite attractive for a scientific understanding of functionalities led by charges.

An example clearly showing the advantage of KFM is the study carried out by Lian *et al* wherein they visualized the potential gradient of planar Schottky heterojunctions [39]. They estimated the surface barrier heights of $Al_{0.22}Ga_{0.78}N$ (29 nm)/GaN and Ni–Si-doped n-GaN (density of n-type dopant of Si: $\sim 3.5 \times 10^{17}$ cm^{-3}) by using KFM. Using comparative CPD mapping (figure 1) in the dark and when illuminated by a monochromatized mercury lamp ($\lambda = 364.5$ nm), the diffusion length of minority carriers at the heterojunction can be evaluated with greater accuracy and higher spatial resolution using KFM rather than a conventional method such as the electron-beam-induced current (EBIC) technique [40, 41]. They found the minority carrier diffusion length in n-GaN near the Schottky junction to be $\sim 1.8 \pm 0.4$ μm. Their results are notable since the accuracy of the estimated diffusion length is of the order of nanometres. They pointed out that the spatial resolution of this technique is determined by the interactions between the tip and the sample and estimated the spatial expansion of the interactions at $\sim$20 nm [42].

The nanoscale visualization of electric properties in a microscopically selected device has attracted the attention of many researchers [43–47]. With the recent technical developments reducing device sizes, the pioneers in this field are keen to obtain the deterministic number of charges and to statistically determine the charge behaviours from the electric potential distribution obtained by KFM. Quantitative charge counting has never been established as a standard technique in SPM measurements. However, local observations of a small number of static charges (which is obviously different from the current resulting from charge flow) has already been observed in various situations, e.g. visualization of charges confined in defects, nanostructures, memory devices, etc.

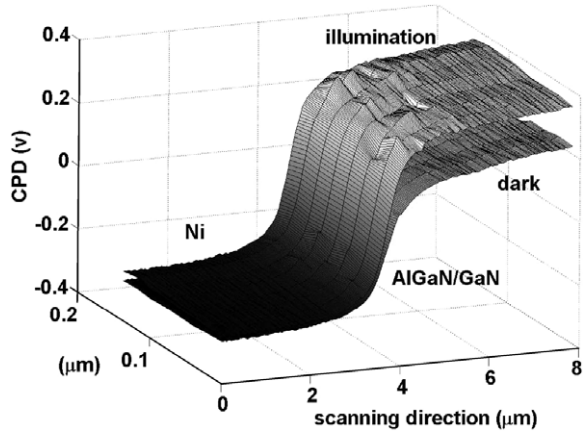

Figure 1. Surface potential distribution across an Ni–GaN junction in dark (bottom) and under 364.5 nm illumination (top). (From figure 2 in [39]. Reprinted with permission from [39]. Copyright 2006, American Institute of Physics.)

2.2. Remaining charges in memory devices

The charges in a flash memory device were observed using a unique SPM system, SNDM, by Cho *et al* [48]. SNDM uses a ring electrode in conjunction with a cantilever to determine the nonlinear dielectric constant. An alternating electric field is applied between the electrode and the sample, and the capacitance distribution on the sample surface is detected as a change in the resonance frequency of an LC (inductance–capacitance) lumped constant resonator [30, 49, 50].

Using SNDM, Cho *et al* successfully visualized the remaining charges in a gate film after writing–erasing cyclic sequences of metal–(SiO_2–Si_3N_4–SiO_2)–semiconductor (metal–ONO–semiconductor, MONOS)-type flash memory [51]. In the MONOS memory, the electrons injected in the write process must be completely neutralized by holes supplied during the erasing process. If the neutralization is incomplete, the memory is filled with the remaining charges and the data is lost. Therefore, a microscopic inspection of the memory (i.e. visualization of the remaining charges after a large number of write–erase sequences) is crucial; the imaging is expected to clarify the mechanism of the undesirable charge remaining in some wrong memory. In their paper on SNDM observations of MONOS, Cho *et al* found specific distributions of remaining electrons that were different from the remaining holes; the electrons had mainly accumulated into the Si_3N_4 layer, while the holes were captured by not only the Si_3N_4 layer but also in the bottom-SiO_2 area. These results suggest

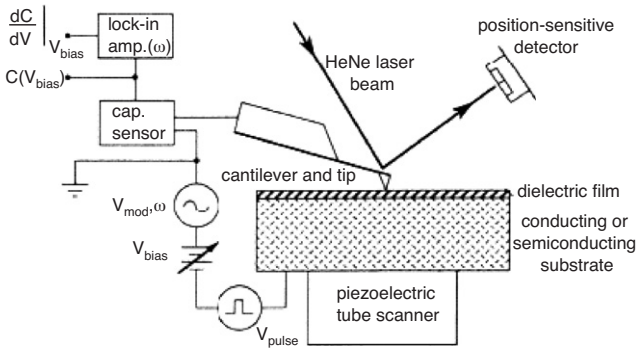

Figure 2. Schematic diagram of the SCM system developed in 1991. (From figure 2 in [52]. Reprinted with permission from [52]. Copyright 1991, American Institute of Physics.)

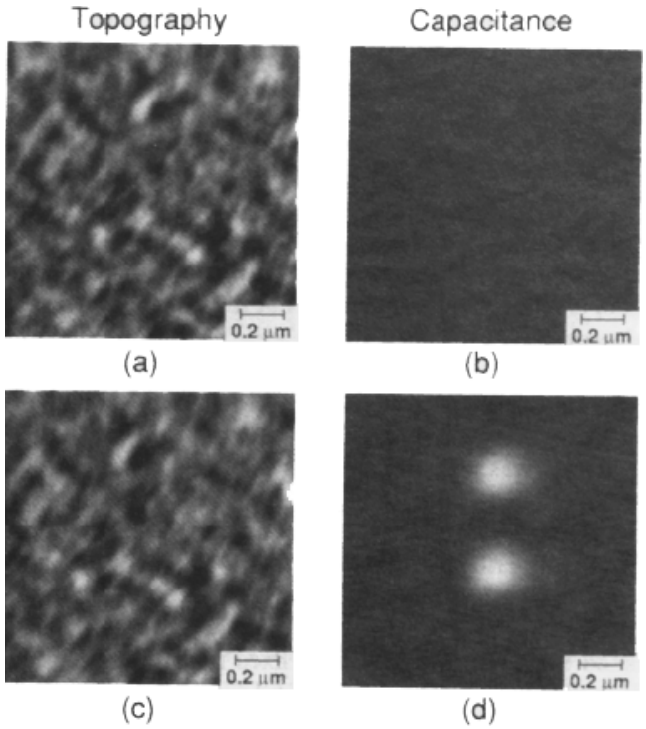

Figure 3. Topography and capacitance images taken before and after writing two charge bits: (a) topography before writing, (b) capacitance before writing, (c) topography after writing and (d) capacitance after writing. Note that the topographic surface does not change by the injection of charges. (From figure 7 in [52]. Reprinted with permission from [52]. Copyright 1991, American Institute of Physics.)

that homogeneously distributed holes partially recombine with heterogeneously distributed electrons. Consequently, the remaining charge distribution in the SNDM image produces a check pattern due to the partial electron–hole recombination in the ONO gate layer. The check pattern had a periodic length of 300 nm.

These researches indicate that static charges can accumulate in few-nanometre-thick films, and SPM can be used to visualize the charge distribution with a horizontal spatial resolution of several tens of nanometres. In general, the spatial resolution is determined by the extension of the electric field from the probing tip. Since the electric field extends over a wider range than the atomic force, the atomic-scale spatial resolution is not easy to achieve in electrical measurements.

3. Observation and control of quasi-static/quasi-dynamic charges

3.1. Development of charge injector and injection properties

Injection, accumulation and removal of charges are the principal operations for data writing, reading and erasing in memory devices. The charge operations in nanoscale areas support ultra-large-scale integration technology. As discussed in this section, a distinctive technique, i.e. charge operation by using a scanning probe, was employed almost simultaneously with charge-sensitive SPM techniques. After this innovation, microscopic charge observation and operation were long believed to be applicable to ultra-high-density memory systems. In fact, the SPM techniques revolutionized the unit of charge packets from the ampere to the coulomb; the charges are not controlled as a large stream of current, but are moved step-by-step from a small area to other neighbouring areas. This is obviously suitable for the digitization of charges.

In this review, the charges in SPM-based memory are categorized as quasi-static/quasi-dynamic charges. For this category, the final states are mainly discussed and the transfer process is not taken into account; this is because the two final states—on and off—are essential for memory and the shortest transfer time possible is required for computing. The discharge process frequently discussed for data volatilization in dynamic random access memory (DRAM) is reviewed in the dynamic charge category.

The SCM technique established in 1991 was developed for analysing two-dimensional charge distributions [52]. The schematic diagram of a capacitance probe system is shown in figure 2. The SCM technique has also been used as an injector of charges. In their first report on SCM, Barrett *et al* reported trapping charges in the nitride–oxide–silicon (NOS) system for visualization and controlling the bias voltage applied to the conductive tip for charge injection and storage (figure 3). The electric field, due to a large bias voltage of +40 V, induced charges in the tunnel through the underlying oxide layer from the Si substrate; these charges are then trapped in the nitride film.

In the developed SCM system, Barrett *et al* used a capacitance pickup circuit from a commercial videodisc recorder as a sensor of the probe [53]. The diversion of the stable and responsive circuit in industrial products would be useful for new applications that demand precise charge operations. The capacitance pickup circuit was also adopted by other groups developing SCM and related systems [54, 55].

As shown in figure 3, Barrett *et al* wrote and erased bit data of charges in an area with a full width at half-maximum (FWHM) of 75 nm. On the basis of the closest packing for the bits with a periodic length of ∼150 nm, the maximum bit density was estimated to be 27 Gbits/inch^2. Unfortunately, this bit density is no higher than that of recently

developed memories, which have extremely high bit densities of the order of Tbit/inch^2 [56]. However, new materials and innovations with a higher capability for bit isolation have been reported in other papers [57, 58]. The details are discussed in section 3.3.

The observation and operation of charges with a scanning probe have been reported for many materials. Charge operations by SPM are a likely candidate for memory systems with Tbit/inch^2 bit density along with other SPM-based data storage techniques [59–61]. The actual use of the system has been debatable because of the property of quasi-static/quasi-dynamic charges, as described below.

To actually use static charges as bit data in DRAM, the access speeds for data reading, writing and erasing, which compete with the bit density, must be investigated. Among these practical factors determining the data access speed, the data-writing speed has been evaluated from the charge injection time necessary for sufficient trapping in the host materials. Tomiye *et al* provided useful information regarding this problem [62]. They stored data in an SiO_2(10 nm)/B-doped Si substrate (p-type 10 Ω cm) by applying a bias of −6 V, indicating that at least 20 ms is necessary for data writing. The charge storage area increases with increasing injection time up to 120 ms and the maximum storage area was estimated to be 1.4 times larger than the actual injected area of 2 μm in diameter. This slow storage should be improved by reducing the bit size; a small bit size can be filled with charges in a short time. However, although they divided the bit area into multiple pixels, Tomiye *et al* still needed time of the order of milliseconds for sufficient charge acquisition at each pixel. Moreover, the expansion of the bit area provided evidence of charge dispersion, i.e. interaction with the neighbouring data.

The SPM-based memory system is highlighted here as a typical application of the SPM charge injector. The problems related to SPM-based memory are ignored for a while. Before looking at solutions, the charge injection in other research fields is introduced. The modulation of electronic states by charge injection into a small area can be considered as local excitation of the site. The responses to the excitation locally characterize the site or induce a specific function in the restricted area. In section 3.2, charge injection is discussed in more general terms to introduce wider applications of quasi-static/quasi-dynamic charges.

3.2. Charge injection at natural sites

As an example of charge injection and its application to defect analyses in devices, Naioto *et al* reported SCM observation of charge trappings for a permittivity (high-*k*) gate stack of titanium oxide–hafnium silicate–silicon oxide (TiO_2/HfSiO/SiO_2) [63]. The charge traps in the high-*k* gate stack are known to induce instabilities at the threshold voltage or trap-assisted leakage current of the transistor [64].

They applied a bias voltage of ±3 V to a 500 nm^2 square area on a TiO_2 (1.4 nm)/HfSiO (∼0.5 nm)/SiO_2 (∼0.5 nm) sample and found a charge trapping state sensitive to the applied bias. The positive bias voltage increases the SCM signal of the state, while the negative bias decreases the signal. The SCM signal changes are dependent on the polarity of the bias and indicate charge trapping and detrapping processes on the high-*k* film. Naioto *et al* also mapped the charging states by using the scanning probe. On the basis of the obtained SCM image, which had a ripple structure with a periodic length of ∼200 nm, positive charges were shown to be trapped heterogeneously on the sample.

A possible origin of the trap centres on the high-*k* film is oxygen vacancies (VO) [65] neutralized by charge trapping and positively charged as VO^{2+} by detrapping. Since VO is formed by the thermal diffusion of Ti atoms, the ripple structure in the SCM image suggests anisotropic Ti diffusion during the film fabrication process.

Charge injection is not specific to certain unique materials but can be confirmed in various insulators. As an unwilling example caused by the injection ability independent of materials, the injected charges are sometimes a competitive and disturbing influence on the main object. The next study is an example of excessive charges in ferroelectric materials that are undesirably introduced by SPM. Its results show that obstinate charges can be found once they settle in the insulator films.

From the concept of realizing DRAM by using charge injection through SPM, SPM-based ferroelectric random access memory (FeRAM) can be deduced [66], which is based on the ferroelectric polarization controlled by SPM. Conventional FeRAM, which is non-volatile, and high-speed memory formed by a ferroelectric capacitor and a field effect transistor (FET), has already attracted the attention of semiconductor companies. In SPM-based FeRAM, the scanning probe is used to access the ferroelectric capacitor instead of the FET.

Although switching of ferroelectric polarization by SPM is expected to be applicable to high-density and non-volatile data acquisition, Son *et al* reported difficulty in separating ferroelectric polarization from the injected surface charges [67]. They fabricated a $BiMnO_3$ ferroelectric epitaxial film on a (111)Pt/TiO_2/SiO_2/Si substrate and applied bias to the SPM probe to induce local ferroelectric polarization. Note that the data-writing process aimed at ferroelectric polarization is the same as that for charge injection discussed in section 3.1. Therefore, both processes are independently induced on the surface. Moreover, for readout of the polarization data, since SPM is operated in KFM mode, the signal showing accumulation of the injected charges is unavoidably convoluted into the signal of ferroelectric polarization at the bit pixel of SPM-based FeRAM.

In order to extract the ferroelectric polarization effect in the bit data, Son *et al* [67] used a zero-biased probe to discharge by surface scanning. In their results, they managed to confirm bit data from ferroelectric polarization and pointed out that the $BiMnO_3$c film had better writing performance compared to $PbZr_{0.53}Ti_{0.47}O_3$ (PZT); this was because of the small surface charge effects due to the semiconducting characteristics of $BiMnO_3$.

After injection, the charges can be stably kept in insulators at room temperature. Tzeng and Gwo injected charges into an Si_3N_4/SiO_2/silicon interface using EFM with a sample

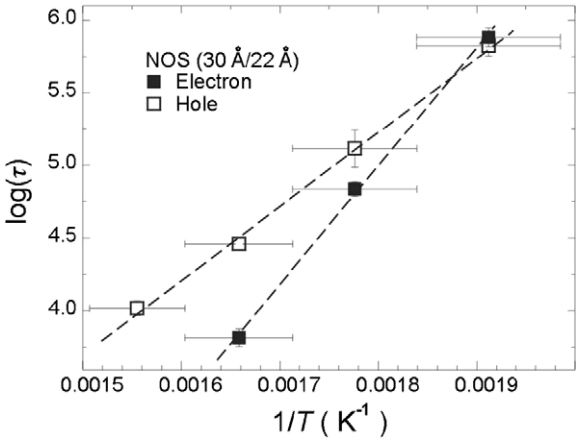

Figure 4. Arrhenius plot of charge retention time for electrons (closed squares) and holes (open squares). From this figure, the trapping energy of the electrons and holes were estimated to be 1.52 ± 0.10 eV and 1.01 ± 0.03 eV, respectively. (From figure 11 in [68]. Reprinted with permission from [68]. Copyright 2006, American Institute of Physics.)

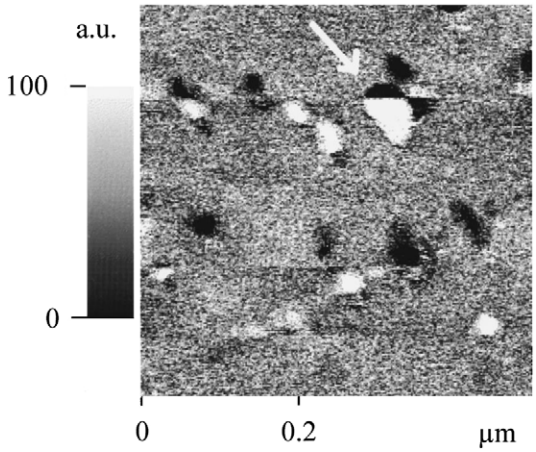

Figure 5. Electrostatic force image of silver nanoparticles on graphite. During the scanning of this image, a DC bias step from +10 to −8 V was applied (at the position indicated by the arrow). It can be recognized that the contrast of the silver particles inverted relative to the background. (From figure 2 in [72]. Reprinted with permission from [72]. Copyright 1997, American Institute of Physics.)

heating system; they found charge decay to be dependent on the sample temperature [68]. Based on EFM observations for various substrate temperatures between 250 °C and 370 °C, the trapping energy of the electrons and holes were estimated to be 1.52 ± 0.10 and 1.01 ± 0.03 eV, respectively (figure 4). These large values suggest that the charges are trapped in deep levels at the interface. They claimed that, if all electrons were trapped at the nitride–oxide interface, the predicted retention time could be around 120 years at 150 °C.

3.3. Charge injection at artificial sites

We now go back to SPM-based DRAM systems. As discussed in section 3.1 with several examples, a common fact is that neither the spatial resolution nor the access speed is high enough for practical use of SPM-based memory systems. In physical terms, the electric field slowly decays with the square of distance to yield a far-field emitting from the tip, which is fatal for high-density data accumulation. For the access speed, the charge trapping centres at the mid-gap level with low charge and discharge rates stabilize the written bit data (see section 3.2), which is not always suitable for reliable data operation at the nanosecond timescale.

In this section, recent trials and suggestions to solve the problems of spatial dispersion and deep trapping levels for charges are reviewed. The basic concept for charge isolation among data pixels is fabricating nanostructures as a 'built-in' pixel array. A built-in pixel with an appropriate energy level (probably not deep) can confine injected charges into a nanoscale area and boost accessibility.

Charge confinement into nanostructures has been reported by Zdrojek *et al* [69]. They injected the charges into conductive nanostructures on insulator thin films and evaluated the charge and discharge phenomena. In this study, the electrically isolated nanostructures, i.e. single-walled carbon nanotubes (SWCNTs), double-walled carbon nanotubes (DWCNTs) and multi-walled carbon nanotubes (MWCNTs), were dispersed by spin-coating onto an SiO_2 thin layer (200 nm) to oxidize an Si substrate. The charges were injected from a negatively biased (−2 to −20 V with respect to the substrate) EFM tip in contact with the nanotube. The charge distribution on the negatively charged nanotubes was observed with EFM in non-contact mode.

They observed highly charged MWCNTs (∼20 nm diameter) after charge injection at ∼−5 V and estimated the linear charge density to be ∼160 electrons μm^{-1}. They found that the injected charges were homogeneously distributed onto MWCNT and that CNT discharged discretely during the EFM scanning, which resulted in step-like heterogeneous charge distributions after several EFM image frames were taken. The spotted CNT suggests that the underlying SiO_2 also contributed to charge trapping. The discharge process depended on the type of CNT: continuous and fast discharges were induced in SWCNTs (∼1 nm diameter) and DWCNTs (∼1.5 nm diameter).

In these experiments, the injected charges were immediately delocalized for CNTs longer than several micrometres [70], indicating that long CNTs are not an ideal material for use as data pixels in memory devices. However, the confinement of charges in the nanostructures in these studies indicates the validity of the built-in pixel concept. For instance, a shortened CNT should be able to act as a high-density built-in pixel.

A similar idea can be found in selective charge storage in nanoparticles, e.g. ∼1.5 nm diameter Co in an SiO_2 thin film [71], 2–3 nm diameter silver on graphite [72] (figure 5), ∼5 nm diameter Fe in SiO_2 [73] and ∼40 nm Si nanoparticles on SiO_2 [34]. In these studies, since high-density nanoparticles were incorporated into the matrix, the charges were injected into multiple particles simultaneously. The common conclusion was that the controllable and reproducible bit size in these high-density systems was estimated to be 20 nm at most. Considering that recent nanofabrication

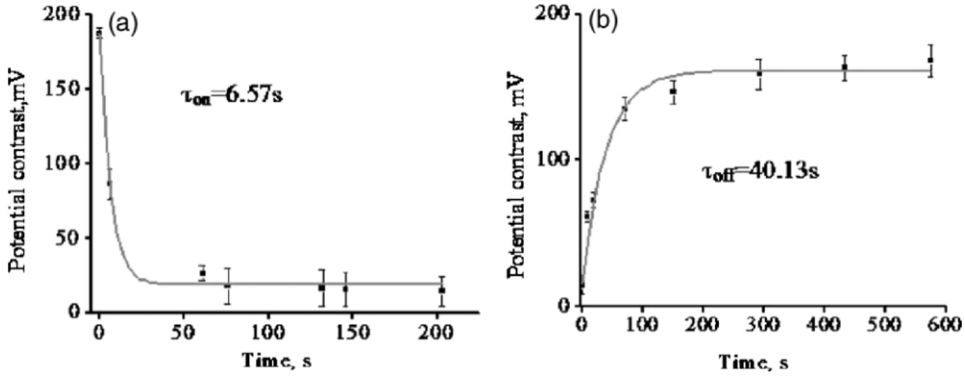

Figure 6. Time dependence of surface potential contrast between $c+$ and $c-$ domains on $BaTiO_3(001)$ surface immediately after UV light was switched (a) on and (b) off. (From figure 2 in [76]. Reprinted with permission from [76]. Copyright 2006, American Institute of Physics.)

techniques can isolate nanoparticles, local charge operations on a single nanoparticle using SPM is a promising technique for the development of an SPM-based memory system.

4. Observation and control of dynamic charges

4.1. Discharge from memory devices

In section 3, various quasi-static/quasi-dynamic charges applicable to memory devices as bit data and electronic analyses of selective sites were introduced. In many studies aimed at charge operations in nanoscale regions, there was a drawback of wide charge dispersion into sub-micron regions on flat surfaces. Delocalization is undesirable, especially for memory media. However, this can hopefully be overcome by using bit pixels defined with nanostructures: the electrically isolated nanostructures can effectively confine the charges without spatial dispersion.

In contrast, the non-dispersive property, i.e. strong charge binding, competes with accessibility to the memory data. When the deep energy level in insulators is used for data accumulation, rapid data operation is difficult to achieve. Therefore, charge dynamics via charge traps in insulator films should be investigated to find an appropriate material for data storage [74, 75]. For practical use of the built-in pixel, more detailed charge dynamics via nanostructures are also required [71].

4.2. Charge redistribution among domains

SPM has the potential for precise charge injection into nanostructures and following the injected charges. This means that SPM can be used as a stand-alone injector/investigator that is not a part of the memory system. Related works on defect analyses were introduced in section 3.2. In this section we discuss other applications, except for the memory system.

In the following discussion, dynamic charges are highlighted because the active charges can directly access the other sites and be a trigger for functions. The dynamic charges introduced here are movable and interactive, unlike the charges in the memory devices. The fast charge transfer indispensable for memory devices is not always required. In fact, for time-resolved SPM analyses to trace dynamic charges, the timescale of the dynamics should be sufficiently longer than the response time involved in SPM systems. For a more precise analysis of the dynamics, the probe should be stopped on a single object, meaning separation from the imaging by the scanning probe. Despite these limitations in the measurements, SPM observations of active charges can reveal the functionality origin and artificially controlled motions in a specific nanoscale area. There have not been many studies on the observation and control of dynamic charges, but the following papers introduce applications of the SPM injector other than memory devices.

Shao *et al* observed the surface potential of a multi-domain $BaTiO_3(001)$ surface using KFM [76] and found that UV irradiation decreases the surface potential due to photo-induced redistribution of charges and their consequent surface screening. In their experiments, when the sample was illuminated by UV light ($\lambda = 254$ nm), a gradual and significant decrease in the surface potential contrast between the $c+$ and $c-$ domains was observed. When the UV was switched off, the potential constant gradually increased back to the original value. They monitored the kinetics of the surface charge redistribution in the presence and absence of light and estimated the time constant of the charge motions to be 6.5 s when the light was on and 40.1 s when it was off (figure 6). These values were explained as the two different processes of photo-excitation and thermal relaxation.

As a related phenomenon, there has been a report that local photochemical reactivity on ferroelectric surfaces depends on the orientation of the domain [77]. In this report, oxidation on into-the-plane polarized domains of $BaTiO_3$ and reduction on out-of-the-plane polarized domains were confirmed. These results indicate that these chemical reactions are closely related to the surface charge and that the specific behaviour of photo-induced charges discovered by Shao *et al* [76] is applicable to nanoscale chemical reaction control. The domain control and the following local charge redistribution induced by SPM or external perturbations should cause alternating local oxidation and reduction at selected sites on the $BaTiO_3$ surface.

The difference in the surface potential between the $c+$ and $c-$ domains on the $BaTiO_3(001)$ surface was also observed with SSPM by Kalinin and Bonnell [78]. They dynamically measured the ferroelectric phase transition of $BaTiO_3$ at the

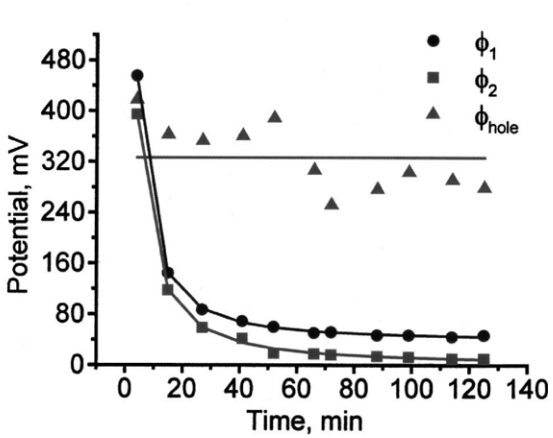

Figure 7. Potential amplitude for two typical domains (closed circles and squares) on $BaTiO_3(001)$ surface observed by time-resolved SSPM. The potential amplitude after the phase transition at 0 min in this figure depended on time. (From figure 8(c) in [78]. Reprinted with permission from [78]. Copyright 2000, American Institute of Physics.)

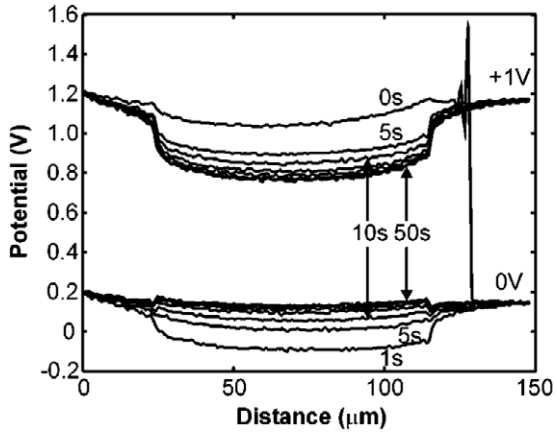

Figure 8. Time-resolved SKPM measurements of potential profile in inkjet-printed PEDOT:PSS. (From figure 2 in [80]. Reprinted with permission from [80]. Copyright 2004, American Institute of Physics.)

Curie temperature T_C = 130 °C using SSPM; they found that potential features of domains are strongly amplified immediately after the phase transition and slowly decay at a timescale of ∼20–30 min (figure 7).

This study indicates that the temperature can be a trigger for inducing the dynamic motion of charges, and time-resolved SPM measurement can reveal the dynamics of the charges.

4.3. Charge redistribution in films

Cao *et al* reported the charge redistribution induced in organic systems due to photon irradiation [79]. They observed the surface potential of an organic layer by KFM combined with a laser (632.5 nm) as a light source to induce the charge redistribution. The organic layer was composed of two dyes (1:1 wt%)—chloroaluminum phthalocyanine (AlClPc) and *N*,*N*8-dioctadecyl-3,4,9,10-perylene tetracarboxylicdiimide (PTCDI-C18H)—and was cast onto a TiO_2 surface. Under illumination, the surface potential was boosted throughout the AlClPc/PTCDI-C18H composite layer and provided uniform features in the KFM image. On the other hand, the KFM image in the dark indicated a high contrast, reflecting surface features. The effect of illumination was explained by photo-induced electron transfer from the AlClPc/PTCDI-C18H composite underlying the TiO_2 layer.

Using time-resolved SKPM, Taylor *et al* observed a reversible polarization process at an interface of indium tin oxide (ITO) electrodes with inkjet-printed polyethylene-dioxythiophene:polystyrene sulfonic acid (PEDOT:PSS) [80], which has been used for defining source and drain electrodes in polymer FETs [81] and write-once–read-many-times (WORM) memory [82]. They found that a space charge in electrodes accumulates and dissipates with a slow time constant of approximately 12 s (figure 8) and concluded that the process was caused by the drift of Na^+ and/or H^+ ions in the polymer.

Obviously, the slow drift of positive ions is profitable to the time-resolved measurement of potential distributions in a large device; note the observed distance between ITO electrodes was ∼100 mm (figure 8).

For time-resolved measurements of SPM, the mechanical response of the scanning probe and electrical response of the signal detection system are crucial factors. Consequently, the actual application is limited to slow phenomena, as discussed in sections 4.1 and 4.2.

4.4. Charge interaction with surroundings

Finally, we review how dynamic charges interact with their surroundings. The charge motions should depend on an external electric field so that the functionality owing to the charges can be locally controlled by an electrically biased SPM tip that approaches nearby sites with local charges.

The approaching SPM tip is known to selectively induce oxidation on the surface, which is referred to as field-induced oxidation (FIO) [83]. Pingree *et al* developed laser-assisted FIO nanopatterning of (111)-oriented hydrogen-passivated silicon surfaces (H:Si(111)) with an atomic force microscope (AFM) [84]. They found that the local oxidation on H:Si(111) surfaces can be drastically accelerated by a laser illuminating a lightly doped and electrically biased silicon cantilever of AFM. This finding is highly applicable and can be attributed to free carrier concentration in the AFM probe by laser irradiation. The carrier concentration induces an additional electric field at the AFM tip, which results in the enhancement of FIO. They achieved nanopatterning of the oxide by toggling the laser: the oxide film is only formed when the laser is on, while the Si bare surface remains when the laser is turned off.

Ng *et al* discussed the interactions of accumulated charges in nanoparticles with their surroundings [35]. They prepared two types of samples—4 nm diameter silicon nanocrystals (nc-Si) with different depth distributions in SiO_2 films—and investigated the dynamics of the charges injected from an EFM tip. They found that the charges in nc-Si near the surface

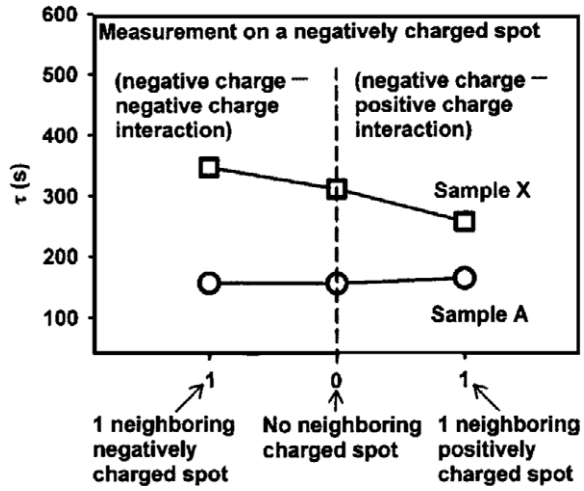

Figure 9. Influence of surrounding charges on discharge process of nc-Si in deep regions. The vertical axis indicates the discharge time constant evaluated from the time-resolved EFM signal. For nc-Si in deep regions (sample X), the rate of negative charge diffusion is increased by the positive charges on the surrounding particles. (From figure 4 in [35]. Reprinted with permission from [35]. Copyright 2005, American Institute of Physics.)

are difficult to keep in the SiO_2 film but easy to discharge into the air, while those in nc-Si in deep regions are easy to diffuse into SiO_2 but difficult to discharge. These contrasting results indicate that the charge behaviour depends on the atmosphere surrounding the nanoparticles; nc-Si on the surface can discharge to humid air, but nc-Si in SiO_2 films tends to maintain the charges without complete discharge into the air. They also found that the diffusion rate of charges from nc-Si in deep regions is affected by the surrounding charges. nc-Si surrounded by negatively charged nanocrystals induces a slow diffusion rate for additionally injected negative charges but a faster diffusion rate for additional positive charges (figure 9). These phenomena can be understood on the basis of electrical repulsive and attractive forces being dependent on the polarity of secondary injected charges.

5. Summary and prospects

Various charge motions, i.e. static, quasi-static/quasi-dynamic and dynamic motions, that locally functionalize materials were reviewed. For microscopic analyses of motions in nanomaterials, scanning probe microscopy (SPM) is sensitive to the charges and is one of the most appropriate tools.

After successful visualization of static charges in electronic devices by SPM, the diagnostics in a single device by SPM has been demonstrated routinely in many sites. The spatial resolution of the static charge observation has been determined by electrical interactions between the tip and charges. Since electrical interactions extend to a wider range than the atomic force, the distinguishable charges in SPM images should be separated by at least 20 nm.

Since the maximum density of the charge array corresponds to the bit density of a Tbit/inch^2-class memory, research on charge operations for an SPM-based memory system has been significantly accelerated. In the system, SPM should play three roles: data writing, reading and erasing. In addition to observing the charges for the data reader, these roles were performed by controlling the bias voltage applied to the probes. At this stage, the charges in the SPM image do not inactively stay in a site but activate in response to the stimulation from the SPM probe. The charges in the memory system must be operated over a short distance as quickly as possible. The quasi-static/quasi-dynamic charges injected into flat insulators occasionally expand widely and get trapped in deep energy levels, which is not desirable for quick operations. Therefore, the system has currently been modified for charge introduction into nanostructures, e.g. nanotubes and nanoparticles, as built-in data pixels.

The accessible electrical states of the nanostructures sometimes compete with the volatility of the data. For an SPM-based memory system, the behaviours of dynamic charges dispersed from nanostructures must be investigated.

In addition to these improvements in memory materials, recent research on fast AFM with a video rate of almost ∼40 ms/frame (100 pixels × 100 pixels) [85–87] has suggested the applicability of the SPM probe to a head arm in the memory to freely access the data pixels. Another study on precisely tuned EFM successfully realized a high spatial resolution at the ångström level [88], indicating that a custom SPM probe can act as a charge operator for high-density media greater than Tbit/inch^2.

The observation and operations of charges by SPM can clarify charge and discharge processes in nanoscale regions, so other applications other than SPM-based memory have been demonstrated. In analytical applications, charge transfer processes which have never been discussed for quasi-static/quasi-dynamic charges in memory devices were highlighted. For instance, time-resolved analyses have revealed the charge redistribution process under illumination. Although the timescale of the analysis was limited by the response time of the SPM system of several seconds, several materials with slow time constants, such as ion diffusion, were successfully analysed. The fast-AFM system with a high response time described above [85–87] would be applicable to the time-resolved analyses of the dynamic charges. The high response time with a moderate spatial resolution is a choice for the particular application. In fact, once an object is selected by the scanning probe, the fixed probe can reveal precise charge motions of the object.

The dynamics of chemical reactions are one of the next research targets for charge-sensitive SPM. In general, chemical properties are difficult to observe by SPM. However, considering that the charge transfer induces chemical functionality, dynamic charge observation may trace the reaction process [89, 90].

This review mainly discussed the spatial and time resolutions in charge observations using SPM. Other SPM applications using the charge transition between an inner shell and a valence shell and its application to local structure analyses [91, 92] were remarked upon as a postscript.

References

[1] Sze S M 1985 *Semiconductor Devices, Physics and Technology* 2nd edn (New York: Wiley)

[2] Grove A S 1967 *Physics and Technology of Semiconductor Devices* (New York: Wiley)

[3] Mitchel W C and Perrin R E 1990 Temperature dependence of the persistent photocurrent in Czochralski gallium arsenide *Phys. Rev.* B **41** 12086–91

[4] Chadi D J and Chang K J 1988 Theory of the atomic and electronic structure of DX centers in GaAs and $Al_xGa_{1-x}As$ alloys *Phys. Rev. Lett.* **61** 873–6

[5] Krause R, Saarinen K, Hautojärvi P, Polity A, Gärtner G and Corbel C 1990 Observation of the monovacancy in the metastable state of the EL2 defect in GaAs by positron annihilation *Phys. Rev. Lett.* **65** 3329–32

[6] Branz H M 1988 Charge-trapping model of metastability in doped hydrogenated amorphous silicon *Phys. Rev.* B **38** 7474–9

[7] Manasreh M O, Mitchel W C and Fischer D W 1989 Observation of the second energy level of the EL2 defect in GaAs by the infrared absorption technique *Appl. Phys. Lett.* **55** 864–6

[8] Nabity J C, Stavola M, Lopata J, Dautremont-Smith W C, Tu C W and Pearton S J 1987 Passivation of Si donor and DX centers in AlGaAs by hydrogen plasma exposure *Appl. Phys. Lett.* **50** 921–3

[9] Plano M A, Plano W E, Haase M A, Bose S S, Holonyak N Jr and Stillman G E 1988 Generation of an anomalous hole trap in GaAs by As overpressure annealing *Appl. Phys. Lett.* **52** 1077–9

[10] Campbell A C, Dodabalapur A, Crook G E and Streetman B G 1989 Study of the DX center fine structure in ion-implanted $Al_{0.27}Ga_{0.73}As$ processed by rapid thermal annealing *Appl. Phys. Lett.* **54** 727–9

[11] Paloura E C, Lagowski J and Gatos H C 1991 New application for isothermal capacitance transient spectroscopy: identification of tunneling in semiconductor–insulator interfaces *Appl. Phys. Lett.* **58** 137–9

[12] Lootens D, Van Daele P, Demeester P and Clauws P 1991 Study of electrical damage in GaAs induced by $SiCl_4$ reactive ion etching *J. Appl. Phys.* **70** 221–4

[13] Monakhov E V, Kuznetsov A Yu and Svensson B G 2001 Vacancy-related deep levels in n-type $Si_{1-x}Ge_x$ strained layers *Phys. Rev.* B **63** 245322

[14] Tomiye H, Yao T, Kawami H and Hayashi T 1996 Nanometer-scale characterization of SiO_2/Si with a scanning capacitance microscope *Appl. Phys. Lett.* **69** 4050–3

[15] Higgins R J, Martin K P, Syphers D A, Van Vechten J A and Palmateer S C 1987 Mobility enhancement of modulation-doped materials by low-temperature optical annealing of spacer-layer defect charge state *Phys. Rev.* B **36** 2707–12

[16] Linke R A, Redmond I, Thio T and Chadi D J 1998 Holographic storage media based on optically active bistable defects *J. Appl. Phys.* **83** 661–73

[17] Villeneuve P R, Abrams D S, Fan S and Joannopoulos J D 1996 *Opt. Lett.* **21** 2017–9

[18] MacDonald R L, Linke R A, Chadi J D, Thio T, Devlin G E and Becla P 1994 Thick plasma gratings using a local photorefractive effect in CdZnTe:In *Opt. Lett.* **19** 2131–3

[19] Lang D V, Logan R A and Jaros M 1979 Trapping characteristics and a donor-complex (DX) model for the persistent-photoconductivity trapping center in Te-doped $Al_xGa_{1-x}As$ *Phys. Rev.* B **19** 1015–30

[20] He Y, Dulub O, Cheng H, Selloni A and Diebold U 2009 Evidence for the predominance of subsurface defects on reduced anatase TiO_2(101) *Phys. Rev. Lett.* **102** 106105

[21] Stroppa A, Duan X, Peressi M, Furlanetto D and Modesti S 2007 Computational and experimental imaging of Mn defects on GaAs(110) cross-sectional surfaces *Phys. Rev.* B **75** 195335

[22] Watanabe H, Baba T and Ichikawa M 1999 Characterization of local dielectric breakdown in ultrathin SiO_2 films using scanning tunneling microscopy and spectroscopy *J. Appl. Phys.* **85** 6704–10

[23] Feenstra R M, Vaterlaus A, Woodall J M and Pettit G D 1993 Tunneling spectroscopy of midgap states induced by arsenic precipitates in low-temperature-grown GaAs *Appl. Phys. Lett.* **63** 2528–30

[24] Trenkler T, Stephenson R, Jansen P, Vandervorst W and Hellemans L 2000 New aspects of nanopotentiometry for complementary metal–oxide–semiconductor transistors *J. Vac. Sci. Technol.* B **18** 586–94

[25] Ballif C, Moutinho H R and Al-Jassim M M 2001 Cross-sectional electrostatic force microscopy of thin-film solar cells *J. Appl. Phys.* **89** 1418–24

[26] Puntambekar K P, Pesavento P V and Frisbie C D 2003 Surface potential profiling and contact resistance measurements on operating pentacene thin-film transistors by Kelvin probe force microscopy *Appl. Phys. Lett.* **83** 5539–41

[27] Nichols J A, Gundlach D J and Jackson T N 2003 Potential imaging of pentacene organic thin-film transistors *Appl. Phys. Lett.* **83** 2366–8

[28] Kalinin S V and Bonnell D A 2002 Scanning impedance microscopy of an active Schottky barrier diode *J. Appl. Phys.* **91** 832–9

[29] Ankudinov A V, Evtikhiev V P, Ladutenko K S, Rastegaeva M G, Titkov A N and Laiho R 2007 Kelvin probe force and surface photovoltage microscopy observation of minority holes leaked from active region of working InGaAs/AlGaAs/GaAs laser diode *J. Appl. Phys.* **101** 024504

[30] Cho Y, Kazuta S and Ito H 2001 Scanning-nonlinear-dielectric-microscopy study on periodically poled $LiNbO_3$ for a high-performance quasi-phase matching device *Appl. Phys. Lett.* **79** 2955–7

[31] Park J Y, Ogletree D F, Thiel P A and Salmeron M 2006 Electronic control of friction in silicon pn junctions *Science* **313** 186

[32] Qi Y, Park J Y, Hendriksen B L M, Ogletree D F and Salmeron M 2008 Electronic contribution to friction on GaAs: an atomic force microscope study *Phys. Rev.* B **77** 184105

[33] Yoshida C, Yoshida A and Tamura H 1999 Nanoscale conduction modulation in Au/Pb(Zr, Ti)O_3/$SrRuO_3$ heterostructure *Appl. Phys. Lett.* **75** 1449–51

[34] Mélin T, Deresmes D and Stiévenard D 2002 Charge injection in individual silicon nanoparticles deposited on a conductive substrate *Appl. Phys. Lett.* **81** 5054–7

[35] Ng C Y, Chen T P, Tse M S, Lim V S W, Fung S and Tseng A A 2005 Influence of silicon-nanocrystal distribution in SiO_2 matrix on charge injection and charge decay *Appl. Phys. Lett.* **86** 152110

[36] Kalinin S and Gruverman A 2006 *Scanning Probe Microscopy: Electrical and Electromechanical Phenomena at the Nanoscale* (New York: Springer)

[37] Bonnell D 2000 *Scanning Probe Microscopy and Spectroscopy: Theory, Techniques, and Applications* (New York: Wiley–VCH)

[38] Meoded T, Shikler R, Fried N and Rosenwaks Y 1999 Direct measurement of minority carriers diffusion length using Kelvin probe force microscopy *Appl. Phys. Lett.* **75** 2435–7

[39] Lian C and Xing H G 2006 Surface potential measurements on Ni–(Al)GaN lateral Schottky junction using scanning Kelvin probe microscopy *Appl. Phys. Lett.* **88** 022112

[40] Vyvenko O F, Krüger O and Kittler M 2000 Cross-sectional electron-beam-induced current analysis of the passivation of extended defects in cast multicrystalline silicon by remote hydrogen plasma treatment *Appl. Phys. Lett.* **76** 697–9

[41] Walters R J, Romero M J, Araújo D, García R, Messenger S R and Summers G P 1999 Detailed defect study in proton irradiated InP/Si solar cells *J. Appl. Phys.* **86** 3584–9

[42] Sadewasser S, Glatzel T, Shikler R, Rosenwaks Y and Lux-Steiner M C 2003 Resolution of Kelvin probe force

microscopy in ultrahigh vacuum: comparison of experiment and simulation *Appl. Surf. Sci.* **210** 32–6
[43] Hammar M, Messmer E R, Luzuy M, Anand S, Lourdudoss S and Landgren G 1998 Topography dependent doping distribution in selectively regrown InP studied by scanning capacitance microscopy *Appl. Phys. Lett.* **72** 815–8
[44] Edwards H, McGlothlin R, Martin R S, Elisa U, Gribelyuk M, Mahaffy R, Shih C K, List R S and Ukraintsev V A 1998 Scanning capacitance spectroscopy: an analytical technique for pn-junction delineation in Si devices *Appl. Phys. Lett.* **72** 698–701
[45] Kang C J, Kim C K, Lera J D, Kuk Y, Mang K M, Lee J G, Suh K S and Williams C C 1997 Depth dependent carrier density profile by scanning capacitance microscopy *Appl. Phys. Lett.* **71** 1546–8
[46] Huang Y, Williams C C and Wendman M A 1996 Quantitative two-dimensional dopant profiling of abrupt dopant profiles by cross-sectional scanning capacitance microscopy *J. Vac. Sci. Technol.* A **14** 1168–71
[47] Neubauer G, Erickson A, Williams C C, Kopanski J J, Rodgers M and Adderton D 1996 Two-dimensional scanning capacitance microscopy measurements of cross-sectioned very large scale integration test structures *J. Vac. Sci. Technol.* B **14** 426–32
[48] Honda K, Hashimoto S and Cho Y 2005 Visualization of electrons and holes localized in gate thin film of metal SiO_2–Si_3N_4–SiO_2 semiconductor-type flash memory using scanning nonlinear dielectric microscopy after writing–erasing cycling *Appl. Phys. Lett.* **86** 063515
[49] Cho Y, Kazuta S and Matsuura K 1999 Scanning nonlinear dielectric microscopy with nanometer resolution *Appl. Phys. Lett.* **75** 2833–5
[50] Matsuura K, Cho Y and Ramesh R 2003 Observation of domain walls in $PbZr_{0.2}Ti_{0.8}O_3$ thin film using scanning nonlinear dielectric microscopy *Appl. Phys. Lett.* **83** 2650–2
[51] Kimura S and Ikoma H 1999 Fowler–Nordheim current injection and write/erase characteristics of metal–oxide–nitride–oxide–Si structure grown with helicon-wave excited plasma processing *J. Appl. Phys.* **85** 551–7
[52] Barrett R C and Quate C F 1991 Charge storage in a nitride–oxide–silicon medium by scanning capacitance microscopy *J. Appl. Phys.* **70** 2725–33
[53] Palmer R C, Denlinger E J and Kawamoto H 1982 Capacitive-pickup circuitry for videodiscs *RCA Rev.* **43** 194–211
[54] Yamamoto T, Suzuki Y, Miyashita M, Sugimura H and Nakagiri N 1997 Development of a metal patterned cantilever for scanning capacitance microscopy and its application to the observation of semiconductor devices *J. Vac. Sci. Technol.* B **15** 1547–50
[55] Ishii M 2002 X-ray absorption fine structure measurement using scanning capacitance microscope: trial for selective observation of trap centers in ∼nm region *Japan. J. Appl. Phys.* **41** 4415–8
[56] Yamakawa K, Ohsawa Y, Greaves S and Muraoka H 2009 Pole design optimization of shielded planar writer for 2 Tbit/inch^2 recording *J. Appl. Phys.* **105** 07B728
[57] Jones J T, Bridger P M, Marsh O J and McGill T C 1999 Charge storage in CeO_2/Si/CeO_2/Si(111) structures by electrostatic force microscopy *Appl. Phys. Lett.* **75** 1326–8
[58] Son J Y, Bang S H and Cho J H 2003 Kelvin probe force microscopy study of $SrBi_2Ta_2O_9$ and $PbZr_{0.53}Ti_{0.47}O_3$ thin films for high-density nonvolatile storage devices *Appl. Phys. Lett.* **82** 3505–7
[59] Mamin H J and Rugar D 1992 Thermomechanical writing with an atomic force microscope tip *Appl. Phys. Lett.* **61** 1003–5
[60] Cooper E B, Manalis S R, Fang H, Dai H, Matsumoto K, Minne S C, Hunt T and Quate C F 1999 Terabit-per-square-inch data storage with the atomic force microscope *Appl. Phys. Lett.* **75** 3566–8
[61] Tybell T, Paruch P, Giamarchi T and Triscone J-M 2002 Domain wall creep in epitaxial ferroelectric $Pb(Zr_{0.2}Ti_{0.8})O_3$ thin films *Phys. Rev. Lett.* **89** 097601
[62] Tomiye H and Yao T 1998 Investigation of charge trapping in a SiO_2/Si system with a scanning capacitance microscope *Japan. J. Appl. Phys.* **37** 3812–5
[63] Naitou Y, Arimura H, Kitano N, Horie S, Minami T, Kosuda M, Ogiso H, Hosoi T, Shimura T and Watanabe H 2008 Charge trapping properties in TiO_2/HfSiO/SiO_2 gate stacks probed by scanning capacitance microscopy *Appl. Phys. Lett.* **92** 012112
[64] Shiraishi K, Yamada K, Torii K, Akasaka Y, Nakajima K, Konno M, Chikyow T, Kitajima H and Arikado T 2004 Oxygen vacancy induced substantial threshold voltage shifts in the Hf-based high-K MISFET with p + poly-Si gates—a theoretical approach *Japan. J. Appl. Phys.* **43** L1413–5
[65] Robertson J 2006 High dielectric constant gate oxides for metal oxide Si transistors *Rep. Prog. Phys.* **69** 327–96
[66] Auciello O 2006 Science and technology of thin films and interfacial layers in ferroelectric and high-dielectric constant heterostructures and application to devices *J. Appl. Phys.* **100** 051614
[67] Son J Y, Kim Bog G, Kim C H and Cho J H 2004 Writing polarization bits on the multiferroic $BiMnO_3$ thin film using Kelvin probe force microscope *Appl. Phys. Lett.* **84** 4971–3
[68] Tzeng S-D and Gwo S 2006 Charge trapping properties at silicon nitride/silicon oxide interface studied by variable-temperature electrostatic force microscopy *J. Appl. Phys.* **100** 023711
[69] Zdrojek M, Mélin T, Diesinger H, Stiévenard D, Gebicki W and Adamowicz L 2006 Charging and discharging processes of carbon nanotubes probed by electrostatic force microscopy *J. Appl. Phys.* **100** 114326
[70] Paillet M, Poncharal P and Zahab A 2005 Electrostatics of individual single-walled carbon nanotubes investigated by electrostatic force microscopy *Phys. Rev. Lett.* **94** 186801
[71] Schaadt D M, Yu E T, Sankar S and Berkowitz A E 1999 Charge storage in Co nanoclusters embedded in SiO_2 by scanning force microscopy *Appl. Phys. Lett.* **74** 472–4
[72] Nyffenegger R M, Penner R M and Schierle R 1997 Electrostatic force microscopy of silver nanocrystals with nanometer-scale resolution *Appl. Phys. Lett.* **71** 1878–80
[73] Xu F T, Thaler S M, Lopez C A, Barnard J A, Butera A and Weston J L 2005 Stable charge storage in granular thin films *Appl. Phys. Lett* **86** 074105
[74] Ishii M and Hamilton B 2004 Electron trapping at the Si(111) atomic step edge *Appl. Phys. Lett.* **85** 1610–2
[75] Ishii M and Hamilton B 2005 Time transient investigation of photo-induced electron localization at atomic step edges of Si(111) *Appl. Surf. Sci.* **248** 14–8
[76] Shao R, Nikiforov M P and Bonnell D A 2006 Photoinduced charge dynamics on $BaTiO_3$(001) surface characterized by scanning probe microscopy *Appl. Phys. Lett.* **89** 112904
[77] Giocondi J L and Rohrer G S 2001 Spatial separation of photochemical oxidation and reduction reactions on the surface of ferroelectric $BaTiO_3$ *J. Phys. Chem.* B **105** 8275–7
[78] Kalinin S V and Bonnell D A 2000 Effect of phase transition on the surface potential of the $BaTiO_3$(100) surface by variable temperature scanning surface potential microscopy *J. Appl. Phys.* **87** 3950–7
[79] Cao J, Sun J-Z, Hong J, Yang X-G, Chen H-Z and Wang M 2003 Direct observation of microscopic photoinduced charge redistribution on TiO_2 film sensitized by chloroaluminum phthalocyanine and perylenediimide *Appl. Phys. Lett.* **83** 1896
[80] Taylor D M, Morris D and Cambridge J A 2004 Time evolution of the electric field at electrode interfaces with conducting polymers *Appl. Phys. Lett.* **85** 5266–8
[81] Sirringhaus H, Kawase T, Friend R H, Shimoda T, Inbasekran M, Wu W and Woo E P 2000 High-resolution

inkjet printing of all-polymer transistor circuits *Science* **290** 2123–6
[82] Möller S, Perlov C, Jackson W, Taussig C and Forrest S R 2003 A polymer/semiconductor write-once read-many-times memory *Nature* **426** 166–9
[83] Dagata J A, Schneir J, Harary H H, Evans C J, Postek M T and Bennett J 1990 Modification of hydrogen-passivated silicon by a scanning tunneling microscope operating in air *Appl. Phys. Lett.* **56** 2001–3
[84] Pingree L S C, Schmitz M J, Kramer D E and Hersam M C 2007 Laser assisted field induced oxide nanopatterning of hydrogen passivated silicon surfaces *Appl. Phys. Lett.* **91** 073110
[85] Yamashita H, Kodera N, Miyagi A, Uchihashi T, Yamamoto D and Ando T 2007 *Rev. Sci. Instrum.* **78** 083702
[86] Ando T, Uchihashi T, Kodera N, Miyagi A, Nakakita R, Yamashita H and Sakashita M 2006 High-speed atomic force microscopy for studying the dynamic behavior of protein molecules at work *Japan. J. Appl. Phys.* **45** 1897–903
[87] Uchihashi T, Kodera N, Itoh H, Yamashita H and Ando T 2006 Feed-forward compensation for high-speed atomic force microscopy imaging of biomolecules *Japan. J. Appl. Phys.* **45** 1904–8
[88] Uchihashi T, Ohta M, Sugawara Y, Yanase Y, Sigematsu T, Suzuki M and Morita S 1997 Development of ultrahigh vacuum-atomic force microscopy with frequency modulation detection and its application to electrostatic force measurement *J. Vac. Sci. Technol.* B **15** 1543–6
[89] Dagata J A, Perez-Murano F, Martin C, Kuramochi H and Yokoyama H 2004 Current, charge, and capacitance during scanning probe oxidation of silicon. I. Maximum charge density and lateral diffusion *J. Appl. Phys.* **96** 2386–92
[90] Dagata J A, Perez-Murano F, Martin C, Kuramochi H and Yokoyama H 2004 Current, charge, and capacitance during scanning probe oxidation of silicon. II. Electrostatic and meniscus forces acting on cantilever bending *J. Appl. Phys.* **96** 2393–9
[91] Ishii M, Hamilton B, Poolton N R J, Rigopoulos N, De Gendt S and Sakurai K 2007 Nanometer scale x-ray absorption spectroscopy and chemical states mapping of ultra thin oxides on silicon using atomic force microscopy *Appl. Phys. Lett.* **90** 06310
[92] Ishii M, Hamilton B and Poolton N R J 2008 Imaging of charge trapping in distorted carbon nanotubes by x-ray excited scanning probe microscopy *J. Appl. Phys.* **104** 103535